Chapter 2

LITERATURE REVIEW

2.1 Nasal route of drug administration

The nasal mucosa of humans presents a slightly acidic environment with a pH value corresponding to 6.3 and maintenance of this pH warrants the action of ciliary clearance in the nasal cavity. Hence, it is advisable that the pharmaceutical formulations meant to be administered intranasally must have a pH value in the range of 4.5-6.5 to circumvent nasal irritation.

Nasal route of administration has manifested its potentials for therapeutic reasons since ages because respiratory tract represents the prime zone of contact of the foreign particles viz., viruses and bacteria with the body and hence unfurls the gateway for therapeutic agents as well. Initially, the intranasal route of administration was opted as a potential administrative route for imparting local actions in case of infections of the respiratory tract or seasonal rhinitis but at the end of the 20^{th} century it emerges as an alternative route for treating systemic symptoms of cardiovascular indications and after the year 1991 advancements in medical research explored the potentials of intranasal route to deliver therapeutic agents to the central nervous system.

2.1.1 Nasal anatomy

Olfaction represents the main function of nose which is beneficial for animals to search for food, mates, and predators. Besides olfaction nose plays a crucial role in filtration, temperature control, and humidification. Nasal cavity can be understood as two separate areas which run from nostrils to the nasopharynx distinguished into three different parts viz., vestibular, respiratory, and olfactory. Vestibular region represents the opening of nostrils and covers an area equal to approximately 0.6 cm^2 consisting nasal hairs and squamous epithelial cells with few ciliated cells. The respiratory region being the most vascular region corresponds to largest part of the nasal cavity which is basically the lateral region of the nasal cavity covering 150 cm^2. If we compare respiratory region of humans with that of rodents,

then we may conclude that respiratory region of humans corresponds to 80 % to 90 % of the nasal cavity whereas it only constitutes to 50 % in case of rodents. The epithelium of respiratory region is columnar and pseudostratified in nature and incorporates four types of cells viz., goblet cells (mucin secreting cells); non-ciliated columnar cells; ciliated cells; and basal cells. The olfactory region engulfs an area of approximately 10 cm^2. The nasal cavity is further affixed to paranasal sinuses which are basically four paired spaces and are named in correlation to the bone where these are positioned viz., sphenoid sinus, frontal sinus, maxillary sinus, and ethmoid sinus. These sinuses aids in the reduction of head weight, humidifying and cleaning of the inhaled air, and accentuation of the synchronization of speech and sound. Nasal cavity of preclinical animal models like rodents and humans mark significant differences in terms of surface area and approachability of the olfactory epithelium. Rodents have a narrower nasal cavity which in turn makes their olfactory epithelium less approachable. In case of humans, olfactory mucosa can be collected by an ENT surgeon by inducing local anesthesia whereas in case of rodents like rats, it needs to be euthanized to approach the olfactory epithelium prior to removal of the nasal bone. But with advancement of technologies, newer surgical methods are developed where epithelium biopsies in rats can be done without prior euthanization. The volume and length, bend from the nostrils into nasal cavity, presence of septal window, and structure of conchae marks other anatomical differences between species in terms of absorption and nasal uptake.

2.1.2 Olfactory region

Olfactory epithelium represents the upper part of nasal cavity (also known as nasal cleft) which is the primary zone of contact between the body and environment. In humans this region represents an area equal to 10 % of the total area whereas in case of rodents, olfactory region covers an area equal to approximately 50 % of the total area of nasal cavity. Bowman's glands, globose basal cells, and horizontal basal cells constitutes the olfactory

region. A mucus layer secreted by Bowman's glands provide a covering to the epithelium whereas globose basal cells and horizontal basal cells situating in close proximity to lamina propria acts as progenitor cells to other cells. Olfactory receptor neurons (also known as olfactory sensory neurons) are enclosed in olfactory epithelium are bipolar cells and unmyelinated with dendritic extension reaching to the mucosal surface. Cilia situated in the mucosal surface carry olfactory receptors. An axon originating from the cell body of olfactory sensory neurons reaches to the olfactory bulb via cribriform plate of the ethmoid bone. Ethmoid bone basically provides a separation between nasal cavity and brain [37].

2.1.3 Intranasal Drug Delivery Systems against Cancer

Intranasal drug delivery system was explored by many research groups for the treatment of cancer. Chung et.al. delivered ligand-conjugated doxorubicin PLGA nanoparticles via intranasal route targeting glioblastoma. This research group reported that intranasal delivery of ligand-conjugated doxorubicin PLGA nanoparticles inhibited cancer growth in the brain compared to free doxorubicin and induced apoptosis of the brain tumor cells without affecting normal brain cells [38]. They postulated that this intranasal, non-invasive approach to treating brain tumors may be translated to treating other diseases associated with the brain.

Wang et.al. explored whether methotrexate (MTX) administered through the nasal cavity could directly target cerebrospinal fluid (CSF), effectively bypassing traditional barriers like the blood-brain barrier. This study investigated the levels of methotrexate in the blood and cerebrospinal fluid (CSF) of rats to determine if there is direct drug transport from the nasal cavity to the CSF following intranasal administration. MTX was administered either intranasally or intravenously to male Sprague-Dawley rats, with drug concentrations measured from CSF and plasma samples. Results showed that plasma levels were significantly lower, and CSF concentrations were significantly higher, following intranasal

administration compared to intravenous administration. The study concluded that MTX is likely directly transported from the nasal cavity into the CSF in rats [39].

Building on the encouraging results of Wang et. al., Shingaki et. al. conducted further research into the intranasal delivery of methotrexate. Their investigation delved deeper into the efficacy and potential benefits of this administration route for targeting cerebrospinal fluid directly. Comparing the concentrations of MTX in plasma and CSF after intranasal (IN) and intraperitoneal (IP) administration, the researchers found significant direct transport to the CSF and brain following nasal delivery. They also tested the effectiveness of nasal chemotherapy with MTX on tumor-bearing rats, finding it significantly reduced tumor weight compared to non-treatment and IP groups. This suggests that the nose-brain direct transport pathway could be applied to new therapeutic systems for brain tumors and other central nervous system disorders [40].

Another research group evaluated the feasibility and extent of delivering 3H-5-fluorouracil to the brain via the nasal cavity in rats, using cerebrospinal fluid (CSF) as a medium. The study confirmed that 3H-5-fluorouracil concentration in the CSF was significantly higher following nasal administration compared to intravenous injection, indicating direct nasal-to-CSF transport. Various methods, including intravenous infusion, nasal instillation, and nasal perfusion, were used to measure 3H-5-fluorouracil concentration in plasma and the cerebral cortex. Uptake clearance was significantly higher with nasal perfusion than with intravenous infusion, demonstrating effective transnasal drug delivery. The study concluded that nasal application enhanced the brain delivery of hydrophilic drugs like 3H-5-fluorouracil. Comparing plasma and CSF after different administration routes, the study concluded that nasal drug application enhanced 3H-5-fluorouracil delivery to the CSF. 3H-5-fluorouracil is a chemotherapeutic agent used to treat various cancers [41].

Marocco et.al. developed a ferritin-based stimuli-sensitive nanocarrier, The-0504, which is highly biocompatible and water-soluble. They reported that The-0504 can incorporate the potent topoisomerase 1 inhibitor Genz-644282 and can cross the blood-brain barrier (BBB) to specifically target gliomas expressing high levels of the ferritin/transferrin receptor TfR1 (CD71). According to their findings, both intranasal and intravenous administration of The-0504 reduced tumor growth and improved survival rates in glioma-bearing mice. However, intranasal delivery is simpler and less invasive, sparing most healthy tissues [42].

Intranasal administration of a concentrated resveratrol formulation effectively delivered the compound to the lungs was studied by Monteillier et.al.. The formulation was given to A/J mice with chemically induced lung cancer three times a week for 25 weeks. The treatment led to a 27% reduction in the number of tumors and a 45% decrease in tumor volume per mouse. *In vitro* studies suggested that apoptosis might be a key mechanism behind resveratrol's effects. The findings highlight the potential of intranasal delivery to overcome resveratrol's low oral bioavailability and support its further evaluation in clinical trials [43].

Tseng et.al. designed gelatin nanoparticles (GPs) grafted with NeutrAvidin(FITC) on their surface (GP-Av) and then conjugated with biotinylated epithelial growth factor (EGF) to form a core-shell structure (GP-Av-bEGF). These nanoparticles targeted EGF receptors (EGFR) to detect lung adenocarcinoma. *In vitro*studiesshowed higher uptake efficiency in adenocarcinoma cells (A549) compared to normal lung cells (HFL1) due to the abundance of EGFR in A549 cells. Confocal microscopy confirmed cellular internalization and lysosomal entrapment of GP-Av-bEGF in A549 cells. *In vivo* aerosol administration to SCID mice showed specific accumulation in cancerous lung tissue, demonstrating the targeting ability of GP-Av-bEGF both *in vitro* and *in vivo*[44].

A mesoporous silica nanoparticles (MSN)-based drug delivery system was developed for lung cancer treatment via inhalation was studied by Taratula et.al.. This system effectively delivered anticancer drugs (doxorubicin and cisplatin) and siRNA targeting MRP1 and BCL2 mRNA to non-small cell lung carcinoma cells. The MSN were targeted to cancer cells using luteinizing hormone-releasing hormone (LHRH) peptide conjugated via a poly-(ethylene glycol) spacer. The combined delivery of drugs and siRNA led to cell death and inhibition of targeted mRNA, enhancing drug cytotoxicity. Local inhalation of MSN resulted in preferential lung accumulation, reducing systemic circulation and limiting accumulation in other organs. The drug delivery system demonstrated effective treatment potential for non-small cell lung carcinoma [45].

Hence, we can conclude that intranasal drug delivery systems have shown significant potential in the treatment of cancer, particularly for targeting central nervous system cancer and lung cancer. This non-invasive method offers several advantages over traditional systemic delivery routes, including bypassing the blood-brain barrier, reducing systemic side effects, and providing a more direct route to the CNS and lungs [46], [47], [48], [49], [50], [51], [52].

2.2 Prior research art on lung cancer

Tseng et.al. had developed a targeted drug delivery system against lung cancer. The research group formulated gelatin nanoparticles surfaced with NeutrAvidin which was further conjugated to epithelial growth factor. The nanoparticles had an average particle size of 220 nm with a zeta potential value of -9.3 mV. The *in vitro* cell line studies were performed on A549 lung cancer cell lines and HFL1 normal lung cell lines and the research group reported that these functionalized gelatin nanoparticles had resulted in better dose and time-dependent cellular uptake in A549 cell lines as compared to normal lung cell lines HFL1 and the reason

that could be accounted for this is the presence of higher amounts of epidermal growth factor receptor in A549 cells. Confocal microscopy further validated the cellular uptake of these functionalized gelatin nanoparticles and depicted the same results. Results from the *in vivo* studies in severe combined immunodeficient mice model revealed drug targeting efficiency of the formulated functionalized gelatin nanoparticles to the lung cancerous cells followed by its accumulation. The researchers concluded that epithelial growth factor conjugated NeutrAvidin gelatin nanoparticles have the potential to be explored for anticancer application [53].

The toxicity profile of anionic clay and nanoparticles of layered metal hydroxide was studied in A549 lung cancer cell lines, normal human lung epithelial L-132 cell lines, HOS (osteosarcoma cell lines), and HeLa (cervical adenocarcinoma cell lines) by Choi et.al. The inorganic nanoparticles resulted in minimal cytotoxic effects at a concentration of less than 250 µg/mL on the viability and proliferation of all four cell lines studied for 48 hours. However, 72 hours of treatment with higher concentrations ranging between 250 to 500 µg/mL had resulted in membrane damage along with oxidative stress-mediated inflammatory response in the order A549> HOS> HeLa cell lines. The research group reported that the toxicity mechanism exhibited by anionic clay or layered metal hydroxide nanoparticles is different from silica nanoparticles, single-walled carbon nanotubes, and iron oxide. Membrane damage-mediated cell death was reported in the case of iron oxide nanoparticles whereas an inflammatory response had been observed for silica nanoparticles, but the extent of cell death is not significant in cancerous as well normal cells in the case of silica. Apoptosis mediated by oxidative stress was observed in single-walled carbon nanotubes. L-132 cell lines were unaffected in terms of cytotoxicity by nanoparticles of layered metal hydroxide at a concentration of less than 250 µg/mL. The research group postulated that

anionic clay and nanoparticles of layered metal hydroxide can be employed for drug delivery and targeting approaches in the treatment of cancer [54].

Rao et.al. evaluated the potential of inhalable doxorubicin loaded effervescent nanoparticles in the treatment of lung cancer. The formulation was evaluated in *in vivo* tumor model of Balb/c mouse. Blank inhalable nanoparticles, inhalable lactose powder plus free doxorubicin, and suspension of doxorubicin nanoparticles, doxorubicin solution, and saline (all three administered intravenously) were set as control. Kaplan-Meier survival curve depicted that the treatment group received inhalable doxorubicin (30µg) loaded effervescent nanoparticles have better survival rate as compared to groups received other treatments. Control group received intravenous administration of doxorubicin nanoparticles or doxorubicin solution had demonstrated a survival of less than fifty days. Higher cardiac toxicity was marked in the group received inhalable free doxorubicin. The research group reported that pathology results obtained from MRI imaging depicted a marked decrease in the size and number of tumors in the treatment group received inhalable doxorubicin loaded effervescent nanoparticles as compared to other treatment groups. Rao et.al. concluded that such non-invasive approach for the treatment of lung cancer could be a turning point in the way lung cancers are treated [55].

Zhou et.al. had validated the potential of silver nanoparticles for the treatment of lung cancer. The research group prepared the silver nanoparticles by chemical reduction method and used sodium citrate. Briefly, at high temperature, a solution of sodium citrate was injected into the silver nitrate solution resulting in the production of silver nanoparticles. The formulated silver nanoparticles were further characterized by UV-visible spectrophotometry, dynamic light scattering for particle size, and field emission scanning electron microscopy for the morphological characteristics. The research group reported that the spherical shaped silver nanoparticles have depicted an average particle size of 30 nm and concluded that particle size of silver nanoparticles was dependent on the concentration of the reducing agent along with

time of the reaction. The anti-proliferative potential of silver nanoparticles was studied in A549 cell lines and results showed dose and time dependent inhibition in the proliferation of the silver nanoparticles. The scientists concluded that silver nanoparticles serve as a potential candidate for cancer treatment and be explored further for drug delivery application against anti-cancer drugs [56].

Efficacy of taxanes as a chemotherapeutic agent and its role in the radiation therapy in the treatment of lung cancer was evaluated by Jung et.al. The research group formulated taxanes loaded polymeric nanoparticles and its effectiveness as a chemoradio therapeutic agent was assessed by flow cytometry, cellular morphology, and clonogenic assay in A549 lung cancer cell lines and *in vivo* studies in xenograft lung cancer mice model derived from A549 cell lines. Taxanes loaded polymeric nanoparticles depicted an average particle size of 45 nm and freely soluble in water. Results of clonogenic assay showed a higher extent of A549 cell death in the group received both taxanes loaded polymeric nanoparticles and radiation therapy. *In vivo* results depicted better radiotherapeutic efficacy when taxanes loaded polymeric nanoparticles were injected into mice (xenograft lung cancer mice model derived from A549 cell lines) intravenously. The research group concluded that taxanes loaded polymeric nanoparticles had synergistically enhanced the effect of dual therapy i.e. chemotherapy plus radiation therapy and could be explored in the treatment of other cancers as well [57].

Menon et.al. developed targeted polymeric drug delivery system specific to folate receptors against lung cancer. The research team co-loaded gemcitabine and NU7441 which is basically a radiosensitizer into PLGA (polylactic-co-glycolic acid) and poly (N-isopropylacrylamide)-carboxymethyl chitosan-based nanoparticles and evaluated their efficiency as a chemoradio therapeutic agent in lung cancer model. The *in vitro* results showed promising hemocompatibility and cytocompatibility with acceptable stability in

alveolar type I cells and dose dependent cellular uptake. Whereas*in vivo* results depicted that the group received gemcitabine and NU7441 co-loaded polymeric nanoparticles had reduced number of tumors in the lung and very low toxicity. Menon et.al. concluded that these folate receptor targeted nanoparticles could be employed effectively for their chemotherapeutic effect along with radio-sensitization action [58].

Munaweera et.al. developed an innovative treatment against lung cancer based on magnetic nanoparticles and external magnetic field mediated delivery to target lung cancer cells. The research group formulated magnetic nanoparticles loaded with cisplatin and holmium-165 (produce holmium-166 when neutron activated which act as radionuclide). The prepared magnetic nanoparticles were characterized by FTIR, PXRD, EDX, and ICP-MS for particle size, zeta potential, and morphology. The *in vitro* studies were carried out on A549 cell lines and results showed that dual drug loaded magnetic nanoparticles led to more cell death of A549 cells when compared to single therapy and free cisplatin. When the administration of these nanoparticles was mediated through an external magnetic field then an increased lung tumors to liver ratio was reported as compared to in the absence of magnetic field. Further results concluded that this external magnetic field mediated delivery of cisplatin and holmium-165 loaded magnetic nanoparticles to target lung cancer cells inhibited the growth of tumor cells in comparison to control group that received no treatment [59].

Wang et.al. evaluated the efficacy of a phytoconstituent against lung cancer in *in vitro* as well *in vivo* models. The research group formulated sol-gel method based solid lipid nanoparticles loaded with curcumin and characterized for physiochemical characteristics. The average particle size was reported to between 20-80 nm and an IC_{50} value of 4 µM against A549 lung cancer cell lines. An apoptosis rate of 63 % was found in case of curcumin loaded solid lipid nanoparticles against 26 % of apoptosis rate of free curcumin in A549 cell lines. Flow cytometry and immunostaining studies revealed that cell death in A549 cells was associated

mediated via apoptosis. Intraperitoneal injection of curcumin loaded solid lipid nanoparticles inhibited 69.3 % of tumor growth as compared to free curcumin which inhibited only 19.5 % of tumor growth in *in vivo* nude mice xenograft (derived from A549 cell lines) model. The study postulates the effectiveness of curcumin loaded solid lipid nanoparticles as a prognostic approach for the treatment of lung cancer [60].

Rajeshkumar et.al. had demonstrated a green synthesis-based approach for the preparation of Mangifera indica derived zinc oxide nanoparticles which were further characterized for physiochemical characteristics. The spherical shaped zinc oxide nanoparticles had an average particle size between 45-60 nm and XRD and EDX data revealed crystalline behavior with hexagonal quartzite. Cytotoxic studies of zinc oxide demonstrated dose dependent cytotoxicity of A549 cell lines with an IC_{50} value of 25 µg/mL. The cytotoxic results exhibited by zinc oxide against A549 cell lines were found to be comparable with the model drug cyclophosphamide and mediated by free radical scavenging [61].

Toxicity of silver nanoparticles on lung cancer A549 cell lines and DNA damage was studied by Foldbjerg et.al. The research group procured poly vinyl pyrrolidone coated silver nanoparticles from NanoAmor (Houston, United States of America). They evaluated the efficacy of poly vinyl pyrrolidone coated silver nanoparticles and silver ions against A549 cell lines. Results of MTT assay, apoptosis assay (annexin V/propidium iodide method), and flow cytometry depicted a strong correlation between early apoptosis, mitochondrial damage, and the levels of reactive oxygen species. The research group reported that reactive oxygen species mediated the DNA damage in a directly proportional manner and the effect is attenuated by pretreatment with N-acetylcysteine (antioxidant) [62].

Cytotoxicity of silica nanoparticles was studied by Lin et.al. in A549 lung cancer cell lines. The research group reported that silica nanoparticles of particle size 15 nm or 46 nm at a dose

of 10 µg/mL to 100 µg/mL showed dose dependent cytotoxicity against A549 cell lines as compared to crystalline silica for 48 hours. Lin et.al. postulated that cytotoxicity of silica nanoparticles was directly proportional to the dose and exposure time viz., 24, 48, and 72 hours. Levels of glutathione, lactate dehydrogenase, malondialdehyde, and reactive oxygen species was quantified to study the mechanism of cytotoxicity and oxidative stress induced by silica nanoparticles in A549 cell lines. The scientist reported that the levels of reactive oxygen species was increased with a decrease in the levels of glutathione. Moreover, cell membrane damage and lipid peroxidation were mediated by an increase in the levels of lactate dehydrogenase and malondialdehyde. The research group concluded that cytotoxicity induced by silica nanoparticles was associated with the oxidative stress [63].

A research group evaluated the potential of inhalation route to deliver epidermal growth factor receptor targeted magnetic nanoparticles to produce heat at the tumour site when subjected to external magnetic field for the ablation of lung tumor cells. The study was carried out in the orthotopic model of lung cancer in mouse. The research group reported that this treatment approach inhibited growth of tumor in the *in vivo* mouse model and paves the way for effective therapy based on hyperthermia caused by magnetic nanoparticles against lung cancer [64].

Lin et.al. carried out another study similar to silica nanoparticles where they evaluated cytotoxic effects of cerium oxide nanoparticles of average particle size of 20 nm against A549 cell lines. The research group performed sulfo-rhodamine B assay to evaluate cytotoxicity of cerium oxide against A549 lung cancer cell lines at concentrations 3.5 µg/mL, 10.5 µg/mL, and 23.3 µg/mL for 24, 48, and 72 hours. They reported that cytotoxicity was increased in a direct proportion to dose and the time of exposure and reduced levels of α-tocopherol and glutathione mediated the production of reactive oxygen species responsible for the oxidative stress in the A549 cells. The levels of lactate dehydrogenase and

malondialdehyde was reported to be increased as a result of oxidative stress depicting damage of cellular membranes and lipid peroxidation, respectively [65]**.**

2.3 Gemcitabine (GEM)

Gemcitabine (GEM) belongs to the class of pyrimidine analogues, chemically it is 2',2'-difluorodeoxycytidine, which is basically a cytidine analogue with hydroxyl groups on ribose sugar replaced by two fluorine atoms. GEM is one of the globally prescribed anticancer drugs widely used in the treatment of pancreatic cancer along with ovarian cancer, breast cancer, non-small cell lung cancer (NSCLC), and bladder cancer, in a combination with other anticancer agents like cisplatin. The hydrophilicity of GEM limits its diffusion across biological membranes, and is transported via nucleoside transporters present in the membrane to the cells [66].

2.3.1 Mechanism of action of gemcitabine as anticancer agent

Post transportation into the cancer cells, phosphorylation with the aid of deoxycytidine kinase (dCK) enzyme and to some extent by the extramitochondrial enzyme thymidine kinase 2 occurs which determines the fate of GEM in the cancer cells (some studies have reported dCK as enzyme limiting the anti-tumour efficacy of GEM, as deficiency of dCK leads to development in resistance to GEM as observed in *in vitro* models [67], [68]). These reactions are followed by string of phosphorylation reactions which leads to the formation of GEM triphosphate (dFdCTP), the active phosphorylated form is then incorporated into the DNA and RNA which further inhibits the process of DNA synthesis. The enzyme ribonucleotide reductase is inhibited by GEM diphosphate (dFdCDP), the enzyme ribonucleotide reductase has its role in the nucleotide pathway for the management of supply of deoxynucleotides to the tumour cells. The anti-tumour effect of GEM is mediated by incorporation of dFdCTP into the DNA and prevention of DNA repair mechanism by 3'-5'- exonuclease which leads to DNA chain termination and cell cycle arrest in S-phase and ultimately programmed cell

death. When dFdCTP is incorporated into RNA, it inhibits RNA synthesis whereas inhibition of ribonucleotide reductase by dFdCDP induces an emptying of deoxynucleoside triphosphate in the cellular pool which results in obstruction of the pathway involved in de novo DNA synthesis [69], [70], [71].

2.3.2 Pharmacokinetics and metabolism of gemcitabine

GEM is detected in the plasma at around 15 to 30 minutes post intravenous infusion of 30 minutes [72] which results in low blood residence time. GEM undergoes rapid metabolism into its phosphates which accounts for its short half-life ranging from 8 to 15 minutes, therefore the therapeutic concentration is achieved by a continuous supply of intravenous infusion which leads to hematological and renal side effects [73], [74].

Enzyme cytidine deaminase (CDA) shows pervasive expression in liver and plasma at significant high levels which inactivates GEM forming 2',2'-difluoro- deoxyuridine (dFdU), this catabolism reaction contributes to metabolism of GEM by liver and plasma in the body. It has been reported that 10 % of the unchanged GEM undergoes renal filtration by kidney, and more than 90 % of the administered dose is usually recovered within 1 week of administration in urine in the form of dFdU (99 %) or GEM (1 %) [75]. GEM is also degraded by the plasma deaminase and because of its rapid degradation and elimination from the body a large dose of GEM is required to meet the therapeutic efficiency which results in toxic side effects [76].

2.3.3 Prior research art on gemcitabine

Literature demonstrating the efficacy of gemcitabine against lung cancer can be traced back to the late 1980s or early 1990s including many clinical trials evaluating its potential against lung cancer [77], [78], [79]. Phase I trials were conducted in chemotherapy naïve subjects and the maximum tolerated dose of gemcitabine was concluded to be 1250 mg/m^2 administered as an infusion for 30 minutes weekly x 3, every 4 weeks [79]. A phase II trial including 361

subjects was conducted to evaluate the efficacy of gemcitabine as a single agent against lung cancer at a dose of 800-1250 mg/m^2 weekly x 3, every 4 weeks [80]. As verified by the Oncology Review Board, response rates after single-agent treatment with gemcitabine were reported to be more than 20 %. Duration of response was found to be 7.6-12.7 months with a median survival of 8-9 months. No toxicity was found after single-agent treatment with gemcitabine except dose-limiting neutropenia which was reported to be rare even at the highest doses [81]. Some studies also postulate that gemcitabine can enhance the radiosensitivity in solid tumors like NSCLC, pancreas, colorectal, and breast cancer cell lines [82], [83], [84].

A phase II trial was conducted by Crino et.al. to evaluate the efficacy and toxicity of gemcitabine against NSCLC as second-line therapy. Gemcitabine at a dose of 1000 mg/m^2 was given to patients (total of 83 patients with a median age of 63 years) with advanced stage III B or IV NSCLC, once a week x 3, every 4 weeks. As per results reported by the research group, the treatment was well tolerated and 19 % of patients have attained a partial response to it. They concluded that gemcitabine could be used as a second-line treatment in patients who previously received platinum-based therapy as a first-line treatment. Gemcitabine has shown no promising activity without any significant toxicity [85].

The synergistic effect of gemcitabine on cisplatin against non-small cell lung cancer and ovarian cancer cell lines was investigated by a research group from the Netherlands, Moorsel et.al. They studied the effect of the combination of gemcitabine and cisplatin in different ratios against A2780 (human ovarian cancer cell line), H322 (human lung cancer cell line), and Lewis lung cancer cell line (murine). They exposed the cells for the period of 4, 24, and 72 hours with different combination ratios of both drugs and calculated the combination index to evaluate the synergistic effect between these two drugs. A combination index value of less than 1 represents synergism between the groups studied. Moorsel et.al. reported that a

combination index value of less than 1 was obtained in all the specified cell lines after a time period of 4, 24, and 72 hours when cisplatin was fixed at IC_{25} and gemcitabine was varied at IC_{50}, IC_{75}, IC_{90}, and IC_{95}. They reported a synergistic effect between these two drugs in all the cell lines but an additive effect in Lewis lung cell lines after 4 hours of exposure. Next, they fixed gemcitabine at IC_{25} and varied the cisplatin at IC_{50}, IC_{75}, IC_{90}, and IC_{95}. They found a combination index value of less than 1 in all the cell lines after 24 hours of exposure except in Lewis lung cell line and H322 cell lines where these two drugs at the specified ratios have demonstrated an additive effect. Moreover, they reported that cisplatin had augmented the incorporation of gemcitabine in DNA and RNA of the A2780 cell lines and also the incorporation into RNA of all the cell lines. As a concluding remark, they postulated that the synergistic effect between gemcitabine and cisplatin seems to be because of an increase in the formation of cisplatin-based DNA adduct which could be due to modifications in DNA due to the incorporation of gemcitabine in the DNA [86].

Brodowicz et.al. have investigated the difference in the median time to progression of lung tumour when treated with gemcitabine alone as a maintenance therapy or in combination with cisplatin as a first-line treatment. They carried out a randomized phase III trial in lung cancer patients with stage IIIB/IV non-small cell lung cancer. These patients were given a dose of 1250 mg/m^2 of gemcitabine for days 1 and 8 along with cisplatin at a dose of 80 mg/m^2 (day 1), every 21 days. Patients on attaining disease stabilization after initial treatment with gemcitabine plus cisplatin chemotherapy were randomized in 2:1 and received gemcitabine as maintenance therapy for days 1 and 8, every 21 days along with best supportive care (GEM arm or BSC arm). Their findings revealed that the value of median time to progression was found to be 5.0 and 6.6 months for BSC and GEM arms, respectively, throughout the study. Whereas found to be 2.0 and 3.6 months for the maintenance period. They reported a median overall survival value of 11 months for BSC and 13 months for GEM arms,

throughout the study. A mild toxicity profile with neutropenia was reported as toxicity. They concluded that treatment with gemcitabine as a maintenance therapy after first-line treatment including gemcitabine in combination with cisplatin resulted in marked longer median time to progression as compared with the best supportive care alone [87].

In a clinical trial, Frasci et.al. evaluated the potential of gemcitabine when given along with vinorelbine to improve the quality of life and survival in elderly patients suffering from advanced-stage lung cancer. Subjects with advanced-stage NSCLC aged more than 70 years were randomly allocated to respective arms, each arm had a sample size of 120 patients. Subjects received 30 mg/m^2 of vinorelbine alone or a combination of gemcitabine (1200 mg/m^2) with vinorelbine (30 mg/m^2), on days 1 and 8 for every 3 weeks. They reported that the risk of death was 0.48 for the group receiving the combination of gemcitabine and vinorelbine group as compared to the group receiving vinorelbine alone as determined by multivariate Cox analysis. Combination treatment was reported to delay the symptoms associated with the condition and deterioration of quality of life. The research group concluded that the combination treatment had resulted in better survival as compared to treatment with vinorelbine alone [88].

Shepherd et.al. conducted a phase I trial to investigate the efficiency of gemcitabine in combination with a platinum-based drug that is cisplatin. Both the drugs were given as 30 minutes infusions weekly for 3 weeks providing that two consecutive doses were given with a week's rest. Cisplatin was administered with a dose increment of 25 mg/m^2 to 30 mg/m^2 whereas gemcitabine was given at a dose of 1000 mg/m^2 to 1750 mg/m^2. They found that a dose reduction was required as thrombocytopenia and granulocytopenia were observed frequently after repeated doses. Non-hematological side effects were mild and reversible. Higher episodes of nausea and vomiting were associated with the administration of cisplatin as compared to single-agent therapy with gemcitabine, but these symptoms were controllable

with antiemetics. The study concluded with a 35.7 % response rate for the 28 patients evaluated [89].

Lima et.al. have evaluated the efficacy and toxicity profile of gemcitabine as a single agent or in combination with irinotecan (camptothecin analog) which is a topoisomerase I inhibitor in lung cancer. The research group recommended that a combination regimen including gemcitabine at a dose of 1000 mg/m^2 and irinotecan at 100 mg/m^2 of dose administered on days 1 and 8 for every three weeks can be employed. They also concluded that a dose escalation of irinotecan to 115 mg/m^2 can be employed due to the absence of severe grade IV hematological and non-hematological toxicities. Further studies were warranted [90].

Giovannetti et.al. have investigated the synergistic effect of gemcitabine and pemetrexed in NSCLC cell lines. They studied the synergistic effect on Calu-1, Calu-6, and A549 cell lines at the cellular and genetic level and evaluated the interaction in terms of combination index. They reported that pemetrexed led to a decrease in the phosphorylation of Akt, augmentation in the expression of dCK, and increased apoptosis in Calu-6 and A549 cells along with an increase in the expression of hENT1 (human nucleoside equilibrative transporter 1) in all the three cell lines. Polymerase chain reaction studies revealed that the sensitivity of gemcitabine and dCK expression are correlated and the expression of glycinamide ribonucleotide formyltransferase, thymidylate synthase, and dihydrofolate reductase was correlated to the sensitivity of pemetrexed. The study concluded that the combination of gemcitabine and pemetrexed has a synergistic effect on the NSCLC cell lines and mediated their anti-tumor effect by inducing apoptosis and suppressing the phosphorylation of Akt. Pemetrexed also augments the expression of hENT1 and dCK, the finding suggested that the modulation of gene expression should be considered during the development of combinatorial chemotherapy treatments [91].

A research group from China, Wang et.al. have developed and characterized chitosan and polyethylene glycol-based gemcitabine-loaded nanoparticles against lung cancer. Their study revealed a sustained drug release pattern as exhibited by these gemcitabine-loaded nanoparticles and *in vitro* studies concluded significant cytotoxicity and cellular uptake against lung cancer cell lines [92].

Solid lipid nanoparticles loaded with gemcitabine were formulated and evaluated by a research group, they reported that these solid lipid nanoparticles have demonstrated an entrapment efficiency of more than 70 % with a sustained drug release profile. The biodistribution of solid lipid nanoparticles loaded with gemcitabine was observed to be highest in the liver and spleen which are the main metabolizing organs for gemcitabine. The formulation was found to be stable for three months [93].

Mutairi et.al. have developed oxaliplatin and gemcitabine-loaded solid lipid nanoparticles against lung cancer. These oleic acid-based lipid nanoparticles were characterized and evaluated against lung cancer using cell line studies on A549 cells. The research group reported that the oleic acid-based oxaliplatin and gemcitabine-loaded nanoparticles have markedly decreased the growth of A549 cells in a dose-dependent manner. They finally concluded that the combination of these two drugs administered via oleic acid-based solid lipid nanoparticles can ameliorate the therapeutic potential against lung cancer [94].

Soni et.al. have formulated mannose-based solid lipid nanoparticles and evaluated their anti-tumor efficacy in A549 cell lines. The aim of using mannose in the fabrication of gemcitabine-loaded solid lipid nanoparticles was to improve the cellular uptake of gemcitabine. The research group evaluated the cellular toxicities and cellular uptake in A549 cell lines and postulated that the formulation has resulted in better target-specific delivery along with augmented therapeutic efficiency and safety [74].

2.4 Epigallocatechin -3- gallate (EGCG)

Epigallocatechin-3-gallate (EGCG) is reported to be the most abundant polyphenolic active constituent of green tea, other polyphenols that completes the chemical composition of green tea includes epigallocatechin, epicatechin gallate, and epicatechin. Tea is basically obtained from the shrub Camellia sinensis and its health promoting medicinal properties had already been discovered in the 5th century A.D. Researchers exploring the therapeutic potentials of EGCG have reported its therapeutic effects as antidiabetic, anti-inflammatory, anticancer, and anti-obesity.

Therapeutic properties exhibited by EGCG has been accredited to the polyphenolic structure present in the chemical structure of EGCG with 3 aromatic rings bonded to a 5-member pyran ring. EGCG have 8 free hydroxyl groups which are susceptible to glucuronidation, sulfonidation, and methylation which often leads to attenuation of its biological activity. EGCG has been reported to be unstable at alkaline and neutral pH conditions and shows deprotonation of the hydroxyl groups which results in its rapid degradation. These obvious reasons accounts for the compromised bioavailability of EGCG and other catechins present in green tea in the biological systems [26]. Moreover, the low bioavailability of EGCG could be also accounted to its low solubility in the gastrointestinal fluid combined with its slow and hard absorption rate, and rapid metabolism and elimination from the body [95].

2.4.1 Mechanism of action of EGCG as anticancer agent

EGCG not only acts as a chemopreventive agent but also as a chemotherapeutic agent against a wide array of cancer cell lines. Inhibition of tumorigenesis, proliferation, and angiogenesis has been attributed as the anticancer mechanism exhibited by EGCG. EGCG exhibits its anticancer effects by multiple pathways in different type of cancers. It is reported to down regulate mRNA and protein expression (of MMP-2 matrix metalloproteinases), in case of

MCF-7 breast cancer cell line. MMP-2 matrix metalloproteinases have documented its role in the degradation of basement membrane, metastasis, and angiogenesis. In case of androgen dependent prostate cancer cell line LNCaP, EGCG suppresses the acetylation of androgen receptor and hence exhibits its anticancer effect. EGCG have reported to upregulate miR-210 microRNA and results in attenuated proliferation and anchorage dependent growth in lung cancer cell lines (H1299 and H460), this confirms the potential of EGCG for microRNA targeting. Another pathway that EGCG considers is it upregulates the caspase-3 activity and mitochondrial damage and instigate apoptosis in HT-29 colon cancer cell lines [26]. Hence, it can be concluded that EGCG exhibits its anticancer potentials by affecting multiple pathways involved in the genesis and progression of cancer.

2.4.2 Prior research art on EGCG

Natural products have proven their effectiveness as medicinal agents since the Second Century B.C. as part of Indian traditional medicines that is 'Ayurveda'. Ayurveda is a science dedicated to the potential of natural products as therapeutic agents and has a vast number of Ayurvedic formulations prepared from natural products [96]. Natural products include plant and animal extracts, marine organisms, microorganisms, metabolites of insects, and chemical components found in animals and humans. As per the statistics on the drugs approved by the FDA (Food & Drug Administration, United States) from 1946 to 2019, more than fifty percent of drugs were sourced from natural molecules[97]**.**

The mechanism of inhibition of lung cancer cell growth by EGCG was studied by Wang et.al. The research group studied the targeting efficiency of EGCG to target miRNA (microRNA) in mouse as well as human lung cancer cell lines. They reported that the expression of miR-210 (regulated by HIF-1α) was upregulated by EGCG in mouse as well as human lung cancer cell lines which resulted in decreased cell proliferation and growth. The research group

postulated that the hypoxia response element mediated the miR-210 upregulation. Their results from the affinity binding assay found that EGCG binds with HIF-1α (K_d equal to 53.47 mM), this result demonstrated that EGCG affects hydroxylation of key Pro residues of the oxygen-dependent degradation domain averting the ubiquitination and proteosome mediated degradation dependent on the pro hydroxylation[98].

Shi et.al. have studied the mechanism of the anti-cancer potential of EGCG in lung cancer cells. Their study included the evaluation of the effect of varying concentrations of EGCG on angiogenesis, migration, epithelial-mesenchymal transition, and invasion in the A549 cell lines induced with nicotine. The research group reported that the invasion and migration were prominently suppressed by the EGCG and inhibited the upregulation of vascular endothelial growth factor, HIF-1α, COX-2, p-ERK, vimentin protein levels, and p-Akt. EGCG was also found to reverse the downregulation of levels of β-catenin protein and p53 protein in the A549 cell lines induced by nicotine. The research group reported that the levels of HIF-1α and vascular endothelial growth factor were also found to be suppressed in the *in vivo* studies performed in the A549 xenografts of nude mice (induced by nicotine). They concluded that EGCG has the potential to be deemed as an anti-cancer agent against the treatment of smoking-induced lung cancer.

Ma et.al. have explored the efficiency of EGCG in targeting the signaling pathway of epidermal growth factor receptors. The research group has studied the underlying mechanism of the anti-proliferative action on human lung cancer cell lines which is responsible for its anti-cancer activity. They reported that EGCG induces cell cycle arrest at the G_0/G_1 phase of the cell cycle and suppresses growth. They purportedly reported that EGCG has attenuated the activation of extracellular signal-regulated kinase ½ (ERK1/2), protein kinase (AKT), and epidermal growth factor receptor on short-term exposure whereas long-term exposure to EGCG has also decreased the nuclear localization of epidermal growth factor receptor along

with expression of cyclin D1 gene. Their study concluded that the signaling pathway of the epidermal growth factor receptor might have contributed to the anti-tumor potential of EGCG [99].

Epigallocatechin-3-gallate loaded lecithin and tween-80 based nanoemulsion was prepared by Chen et.al., they evaluated the effect of EGCG on the signalling pathway of AMP-activated protein kinase. The research group carried out *in vitro* cell line studies on H1299 cells, which are lung cancer specific. They studied *in vitro* cytotoxicity, migration, colony formation, and invasion studies and the effect of EGCG on the signalling pathway of AMP-activated protein kinase by western blot studies. They reported that EGCG-loaded nanoemulsion has attenuated the proliferation (IC_{50} value of 4.71 µM), migration, colony formation, and invasion in H1299 cell lines, moreover, they proposed that EGCG modulated the expression of regulatory proteins in the signalling pathway of AMP-activated protein kinase [100].

Another research group has studied the effect of EGCG on the matrix metalloproteinase-2 pathway and subsequently invasion of the CL1-5 lung cancer cell line. Deng et.al. carried out western blot studies, gelatin zymography, RTPCR, transwell migration assay, and flow cytometry analysis (for apoptosis and cell cycle-related studies) and reported that the expression of matrix metalloproteinase-2 in lung cancer cell line CL1-5 had been inhibited by EGCG at the transcriptional level along with downregulation of c-Jun N-terminal kinase pathway which in turn led to the suppression of the transcriptional factors (NF-kB and Sp1). They further studied the synergistic effect of EGCG with the anticancer drug docetaxel and reported that EGCG had synergistically aggravated the anticancer effects of docetaxel in the CL1-5 cell lines. Their cell cycle studies in CL1-5 cell lines revealed that treatment with EGCG had inhibited the proliferation of CL1-5 cells by inducing cell cycle arrest at the G_2/M phase of the cell cycle [101].

Researchers Rawangkan et.al. have studied the effect of EGCG on the expression of programmed cell death ligand 1 in lung cancer A549 cell lines. Their findings revealed that the interferon and epidermal growth factor-mediated expression of programmed cell death ligand 1 was inhibited by EGCG. In A549 cells, the mRNA and protein levels in the interferon-mediated programmed cell death ligand 1 expression were found to be reduced to 40-80 % post-treatment with green tea extract and EGCG through suppression of the JAK2/STAT 1 signaling pathway. Similarly, the expression of programmed cell death ligand 1 mediated by epidermal growth factor was decreased to 37-50 % by EGCG in Lu99 cell lines through the epidermal growth factor receptor and AKT signaling pathway. The research group further studied the effect of EGCG on programmed cell death ligand 1 in A/J mice lung cancer modeland reported that the expression of programmed cell death ligand 1 was decreased to around 70 % (9.6 %- 2.9 %) by EGCG. Their coculture experiments reported that a 30 % reduction in the expression of programmed cell death ligand 1 was found in F10-OVA melanoma cells with a restoration of the expression of interleukin-2 mRNA in CD3+ T cells. The research group concluded that EGCG could act as an immune checkpoint inhibitor [102].

Tang et.al. have reported a unique drug delivery system of EGCG functionalized chitin-based honokiol nanoparticles formulated via the process of ionic crosslinking for the treatment of liver cancer. The research group characterized it for micromeritic properties and reported that spherical-shaped EGCG functionalized chitin-based honokiol nanoparticles had an average particle size of 80 nm with a zeta potential value of + 33.8 mV. The *in vitro* and *in vivo* studies carried out by Tang et.al. have demonstrated a decrease in the proliferation of HepG2 cell lines at the G_2/M phase of the cell cycle mediated by a decrease in the mitochondrial potential of HepG2 cells. EGCG functionalized chitin-based honokiol nanoparticles at a dose of 40 mg/kg were reported to inhibit the 83.55 % tumor growth as compared to 30.15 % by

the free honokiol at the same dose. Based on their results Tang et.al. have postulated the efficacy of EGCG functionalized chitin-based honokiol nanoparticles against liver cancer [103].

Mi et.al. have demonstrated the efficacy of EGCG in combination with doxorubicin for the treatment of gastric cancer by inhibiting the pump P-glycoprotein efflux activity and proliferation of gastric cancer cells. The research group has formulated a gelatin-conjugated polyethylene glycol and hyaluronic acid complex-based nanoparticles co-loaded with EGCG and doxorubicin. The micromeritic studies revealed that the prepared nanoparticles had an average particle size of less than 300 nm with zeta potential values greater than -20 mV. The prepared gelatin conjugated polyethylene glycol and hyaluronic acid complex-based nanoparticles co-loaded with EGCG, and doxorubicin depicted a sustained drug release profile for 24 hours with higher proportions of drug released at pH 6.5 than the physiological pH 7.4. The research group reported that the CD44 ligand recognition study had demonstrated successful uptake of the gelatin-conjugated polyethylene glycol and hyaluronic acid complex-based nanoparticles co-loaded with EGCG and doxorubicin into MKN45 gastric cancer cell lines and suppression of proliferation of cells was mediated by apoptosis (caspase induced) with cell cycle arrest at G_2/M phase of the cell cycle [104].

Similarly, a research group has evaluated the efficacy of EGCG derivatives with the most used anticancer drug cisplatin against lung cancer. Wang et.al. synthesized a series of derivatives of EGCG and their anticancer potential was investigated alone or in combination with the drug cisplatin *in vitro* and *in vivo* models. *In vitro* cytotoxicity assay, apoptosis, and cell cycle distribution were studied in the A549 lung cancer cell line whereas *in vivo* studies were carried out in the NCI-H441 xenograft model. The results from *in vitro* studies revealed that the different derivatives of EGCG had significantly suppressed the proliferation of A549 cells and the formation of colonies, marked apoptosis of cells, and redistribution of the cell

cycle. However, the results obtained for the combination of EGCG derivatives with cisplatin had shown better inhibition of cell proliferation, augmented rate of apoptosis, and redistribution of the cell cycle in comparison to EGCG derivatives alone. The *in vivo* results obtained from the xenograft model revealed a promising reduction in tumor growth. The research group postulated that treatment had attenuated the expression of different genes viz., p-ERK, p-AKT, and p-EGFR, in both *in vitro* and *in vivo* lung cancer models and inhibited the expression of the signalling pathway of EGFR [105].

Another research group has also studied the synergistic effect of EGCG with the drug cisplatin against lung cancer. Chen et.al. had formulated self-assembled gelatin-EGCG nanoparticles loaded with cisplatin. The average particle size was found to be 75 nm with a zeta potential value of +19.83 mV and spherical morphology as observed by transmission electron microscopy. The percent entrapment efficiency for cisplatin in the gelatin-EGCG self-assembled nanoparticles was determined to be 63.7 %. The *in vitro* study on A549 cell lines revealed better cytotoxicity effect (determined by WST-8 cell proliferation assay) and cellular uptake exhibited byself-assembled gelatin-EGCG nanoparticles loaded with cisplatin as compared to cisplatin treatment alone. The research group concluded that this combination treatment could be a successful approach against lung cancer where resistance to cisplatin has occurred [27].

Cromie et.al. have demonstrated the effect of EGCG on the anticancer potential of leptomycin B against lung cancer. Cromie and Gao studied the synergistic effect of EGCG and leptomycin B on lung cancer A549 cell lines and determined the molecular mechanism responsible for their anticancer activity. The study revealed a higher cytotoxicity effect and levels of reactive oxygen species in the treatment group that received a combination of EGCG and leptomycin B as compared to the treatment group that received leptomycin B alone. The molecular studies revealed that the combinatorial therapy of EGCG and

leptomycin B had increased the leptomycin B induces cytotoxicity mediated through the production of reactive oxygen species and the regulation of pathways of p21/surviving and drug metabolism [106].

2.5 Excipients profile

2.5.1 Glyceryl Monostearate ($C_{21}H_{42}O_4$) [107]

IUPAC nomenclature: 2,3-dihydroxypropyl octadecenoate

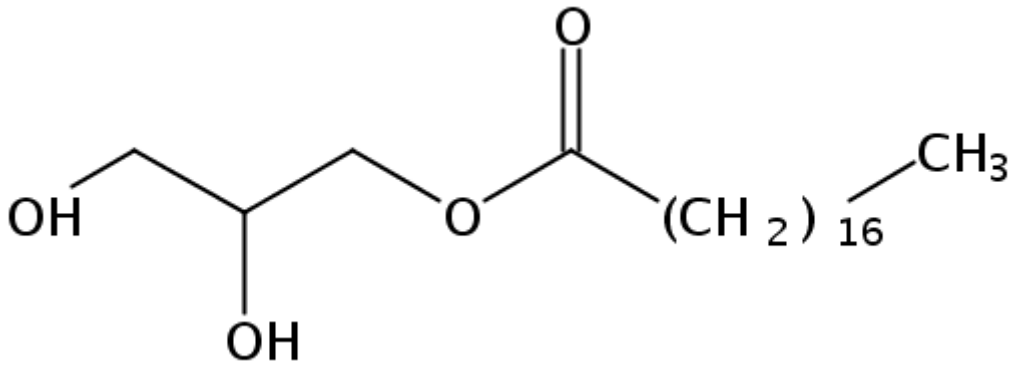

Molecular Properties

- **Molecular Weight:** 358.6 g/mol
- **XLogP3:** 7.4

Physical Description:

The substance can appear in various forms, including other solid, pellets or large crystals, dry powder, and liquid. It is typically described as a white waxy solid but can also be a white to pale yellow wax-like solid with a mild fatty odor. Glycerol monostearate, commonly known as GMS, is the glycerol ester of stearic acid. It is commonly used as an emulsifier in foods.

Solubility:

The substance is insoluble in water. However, it is soluble in hot oils and organic solvents. It also dissolves in hot alcohol, specifically ethanol.

Chemical Classes:

This substance belongs to the class of stearates.

2.5.2 Polyvinyl Alcohol ($C_2H_3OR)n$ where R = H or $COCH_3$[108]

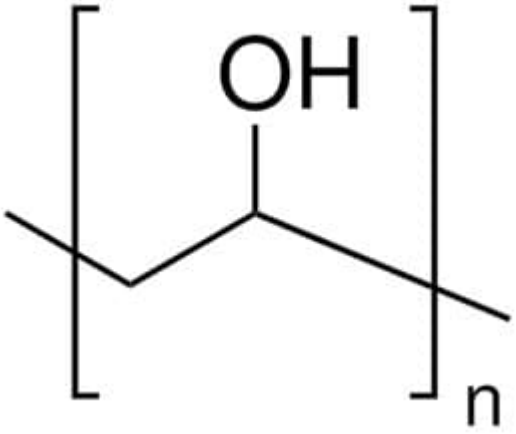

Physical Description:

Polyvinyl alcohol (PVA) appears as odorless white to cream-colored granules or powder. Its pure aqueous solutions are neutral or slightly acidic, with a pH (4% aqueous solution) range of 5-8, and are prone to mold growth. It is strongly hydrophilic.

Solubility:

PVA is a water-soluble synthetic polymer.

Boiling Point:

- Approximately 644 °F (760 mm Hg)

Melting Point:

- Decomposes at 442 °F

- Other melting points range from 212-267 °C

Flash Point:

- 175 °F

Density:

- 1.329 (denser than water, will sink)
- Range: 1.19-1.31 g/cm³

Decomposition:

- Emits acrid smoke and irritating fumes when heated to decomposition
- Decomposes at 228 °C
- Softens at about 200 °C with decomposition

Viscosity:

- 4.8 to 5.8 mPa.s (4% solution at 20 °C) corresponding to an average molecular weight of 26,000-30,000 Da

pH:

- 5.0 to 6.5 (4% solution)

Refractive Index:

- 1.49-1.53

Acid Value:

- Not more than 3.0

Other Experimental Properties:

- Polymer average molecular weight: 120,000
- Subject to mold growth

Uses:

PVA has diverse roles in both commercial and industrial applications, including:

- Papermaking
- Textiles
- Printing

Additionally, PVA is used in ophthalmic solutions as a lubricant to prevent eye irritation or relieve dryness.

Pharmacodynamics:

Polyvinyl alcohol temporarily relieves burning and irritation caused by dry eyes or exposure to wind and sun. It lubricates the eyes and helps protect against further irritation and dryness.

Absorption, Distribution, and Excretion:

Polyvinyl alcohol is poorly absorbed from the gastrointestinal tract and is readily eliminated from the body.

2.5.3 Pluronic F-127 ($C_7H_{16}O_4$) [109]

IUPAC: 2-[2-(2-hydroxyethoxy)propoxy]ethanol

Molecular Properties:

- **Molecular Weight:** 164.20 g/mol
- **XLogP3:** -1

Physical Description:

Pluronic F-127 is a triblock copolymer composed of a central hydrophobic chain of poly(propylene oxide) with 70 units, flanked by two hydrophilic chains of poly(ethylene oxide) with 20 units each. Its molecular formula is $HO[CH_2CH_2O]_2O[CH_2CH(CH_3)O]_{70}[CH_2CH_2O]_2OH$. Pluronic F-127 functions as a nonionic surfactant.

Uses:

Pluronic F-127 is a nonionic polyoxyethylene-polyoxypropylene block copolymer available in various grades, ranging from liquids to solids. It is utilized in several roles, including:

- Emulsifying agent
- Solubilizing agent
- Surfactant
- Wetting agent for antibiotics

Additionally, it is employed in ointment and suppository bases and serves as a tablet binder or coater.

Pharmacological Classification

As Excipients: Inert substances added to medications to ensure the desired consistency of the dosage form. They include binders, matrix materials, bases, or diluents used in pills, tablets, creams, salves, and other formulations. Excipients help provide the necessary texture, stability, and delivery properties for medications.

As Surface-Active Agents: Surface-active agents, or surfactants, alter the interfacial tension of water. These agents typically have one lipophilic (fat-loving) and one hydrophilic (water-

loving) group in their molecule. Examples include soaps, detergents, emulsifiers, dispersing and wetting agents, and some antiseptics. They are used to improve the mixing and spreading of liquids, enhance the absorption of active ingredients, and assist in cleaning and emulsifying tasks.

2.5.4 Hydrogenated soy phosphatidylcholine ($C_{44}H_{88}NO_8P$) [110]

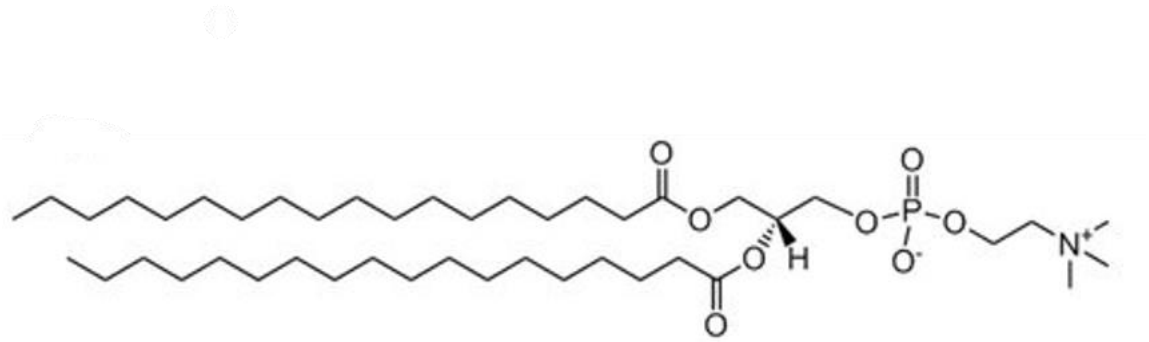

Physical Description:

Hydrogenated Soy Phosphatidylcholine (HSPC) is a saturated phospholipid commonly used in liposomal drug delivery formulations. It enhances the solubility and bioavailability of hydrophobic drugs. HSPC is known for its high oxidative stability and low hygroscopicity, which contribute to improving overall drug efficacy.

Synonyms:

- L-α-phosphatidylcholine (soybean, hydrogenated)
- HSPC

Purity:

- > 98%

Solubility:

- Soluble in chloroform, methanol, ethanol, dichloromethane

Appearance:

- Powder agglomerates

Molecular Weight:

- 790.16 g/mol

Applications:

Drug delivery

2.6 Solid Lipid Nanoparticles (SLNs)

Lipid based drug delivery systems have gained special interest nowadays, but their origin can be traced back to 1965 when liposomes were discovered by biochemist 'Bangham' [111]. The baroque period of lipid-based drug delivery systems from 1980s culminates in the significant advancements in terms of stability of liposomes and introduction of a new lipid-based drug delivery system incorporating solid lipids dispersed in an aqueous system of surfactant in the early 1990s which were referred to as solid lipid nanoparticles (SLNs). This burgeoning period continues till late 1990s when nanostructured lipid carriers (NLCs) came into existence. NLCs are considered as second generation of SLNs which incorporate both solid as well as liquid lipid in their structure.

Solid lipid nanoparticles are colloidal carrier system encompassing solid lipid, water, and surfactant. Solid fat or lipids include fatty acids, waxes, steroids, monoglycerides, diglycerides as well as triglycerides and the limit for their concentration ranges between 0.1-30% w/w of the formulation [111], [112]. Surfactant or emulsifiers of natural origin as well as synthetic have been commonly employed in the formulation of SLNs and their concentration ranges between 0.5-5%, the role of surfactant is to stabilize the formulation and proper selection of solid lipid as well as surfactant affects the particle size, release pattern, drug

loading, and stability of SLNs. The obvious merits of SLNs over nanoemulsions and polymer-based nanoparticles are enhanced stability of the drug, accentuated drug entrapment efficiency and biocompatibility as these are mostly formulated from biodegradable excipients and generally regarded as safe (GRAS) certified excipients. Apart from these merits SLNs also command the encapsulated drug release and averts the premature degradation of the drug in the system [26].

2.6.1 Methods of preparation of SLNs

SLNs can be prepared by employing different methods depending on the characteristics of the drug as discussed. The two commonly employed methods are hot homogenization and cold homogenization [111]. Both methods involve melting of the lipid at a temperature higher than their melting point and the drug is being dissolved in this melt. Hot homogenization is different from cold homogenization in the way drug dissolved lipid melt is allowed to disperse in the hot aqueous solution of surfactant (at the same temperature as the lipid melt) under continuous stirring resulting in the formulation of a pre-emulsion which is further subjected to the process of homogenization with the aid of a homogenizer and leads to the formation of an oil in water nanoemulsion which is cooled and stored. Whereas cold homogenization employs cooling of the lipid melt containing drug which is further emulsified in the cold aqueous surfactant solution followed by homogenization at or at a temperature below the room temperature. Hot homogenization is not an appropriate choice while formulation SLNs of a drug which is hydrophilic in nature because dispersing of hot lipid melt containing drug into hot aqueous surfactant solution may partition the hydrophilic drug between the lipid and aqueous phase. Microemulsification is the commonly employed technique for the formulation of SLNs. In this technique the drug is dissolved in the melted lipid and on the other hand aqueous phase is heated separately isothermally. Surfactant can be added into either aqueous or lipid phase depending upon the conditions. Both the phases are

allowed to mix isothermally followed by plunging in ice cold water under constant stirring. This results in the formation of microemulsified lipid nanoparticles. This method is not apt for formulating thermolabile drugs into SLNs.